

January 01, 2004

Bridging k - and q - space in the cuprates: comparing ARPES and STM results

R. S. Markiewicz
Northeastern University

Recommended Citation

Markiewicz, R. S., "Bridging k - and q - space in the cuprates: comparing ARPES and STM results" (2004). *Physics Faculty Publications*. Paper 46. <http://hdl.handle.net/2047/d20000399>

This work is available open access, hosted by Northeastern University.

Bridging k- and q- Space in the Cuprates: Comparing ARPES and STM Results

R.S. Markiewicz

Physics Department, Northeastern U., Boston MA 02115

A critical comparison is made between the ARPES-derived spectral function and STM studies of Friedel-like oscillations in $\text{Bi}_2\text{Sr}_2\text{CaCu}_2\text{O}_{8+\delta}$ (Bi2212). The data can be made approximately consistent, provided that (a) the elastic scattering seen in ARPES is predominantly small-angle scattering and (b) the ‘peak’ feature seen in ARPES is really a dispersive ‘bright spot’, smeared into a line by limited energy resolution; these are the ‘bright spots’ which control the quasiparticle interferences. However, there is no indication of bilayer splitting in the STM data.

Scanning tunneling microscopy (STM) studies [1,2] in $\text{Bi}_2\text{Sr}_2\text{CaCu}_2\text{O}_{8+\delta}$ (Bi2212) find striking periodic patterns in real-space local density of states (dos) maps. A number of periodicities are found, with different orientations and dispersing with binding energy ω below the Fermi level [2,3]. While a number of models have been proposed for this effect [4–6], here some consequences of a particular quasiparticle interference (QPI) model [7,2] will be explored. The QPI model suggests that the periodicities arise from quasiparticle interference effects, similar to the Friedel-like oscillations observed [8] on clean metal surfaces, near a step edge or point impurity. This model has been extremely successful in predicting an array of periodicities and their dispersions [2,3], and moreover extracting both a Fermi surface $E(\vec{k})$ and a superconducting gap $\Delta(\vec{k})$ which are in good agreement with those found by angle-resolved photoemission spectroscopy (ARPES).

The main issue addressed in the present paper is: are ARPES results consistent with the QPI model? More specifically, whereas normal-state Friedel oscillations are dominated by ‘lines’ – nesting of flat segments of Fermi surface – the superconducting QPI is dominated by ‘points’ – highly localized peaks in the local density of states, herein called ‘bright spots’. While these bright spots provide a detailed explanation for the STM observations, they should be directly observable in the ARPES spectra, and they have not so far been reported. Here it is shown that this could be a result of finite ARPES resolution blurring the bright spots into the quasiparticle peak seen in ARPES in the superconducting state as extending around much of the Fermi surface.

Figure 1 shows an experimental Fermi surface (FS) map of an overdoped Pb-doped Bi2212 sample with $T_c = 70\text{K}$ with strongly suppressed superstructure [9], taken in the superconducting state. The figure shows no trace of the isolated bright spots postulated in the QPI model (compare, e.g., Fig. 3 below). While the STM data are actually taken on more underdoped samples, the overdoped sample was chosen as having much sharper spec-

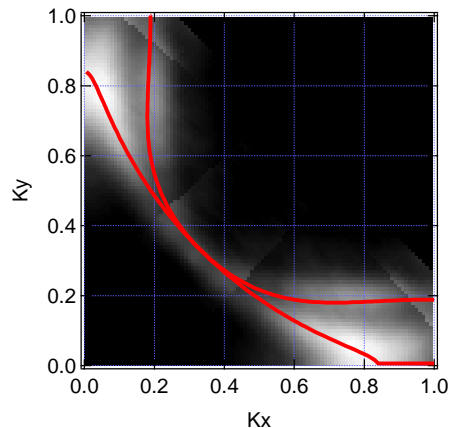


FIG. 1. Experimental ARPES spectral weight at the Fermi level for the sample in the normal state at 100K. Lines show tight binding fit.

tra (including well resolved bilayer splitting [10]), which should make the bright spots easier to see. While the ARPES spectrum is multiplied by a matrix element [11], there is no reason why this should obscure the bright spots.

For modelling purposes, the electronic dispersion is fit, Fig. 1, to the form

$$\epsilon_k = -2t(c_x + c_y) - 4t'c_xc_y - 4t''(c_x^2 + c_y^2 - 1) \pm \frac{t_z}{2}\left(\frac{c_x - c_y}{2}\right)^2, \quad (1)$$

with $c_i = \cos k_i a$, and parameters $t = 0.3\text{eV}$, $t' = -0.11\text{eV}$, $t'' = 0.028\text{eV}$, $t_z = 0.24\text{eV}$, and chemical potential $\mu = -0.44\text{eV}$. While the fit assumes one hole-like and one electron-like FS, the experimental spectra are so broad that comparable fits could be made assuming two hole Fermi surfaces.

A more direct comparison with STM results can be made. Indeed, the Fourier transform of these STM oscillations (which is here called a ‘q-map’) is approximately [7] given by the convolution of the ARPES spectral function at wave number \vec{k} with that at $\vec{k} + \vec{q}$, averaged over \vec{k} (see Eq. 4, below). Figure 2 presents an *experimental* reconstruction of this quantity, derived from convolution of ARPES data at a series of energies $\omega = 2\text{--}12\text{meV}$, below the superconducting gap Δ_0 . These data were taken from the same sample as in Fig. 1; the analysis was kindly carried out by P. Bogdanov [12]. In the direct convolution, these features are superposed upon a large, featureless peak near (π, π) ; to enhance contrast, a derivative of the

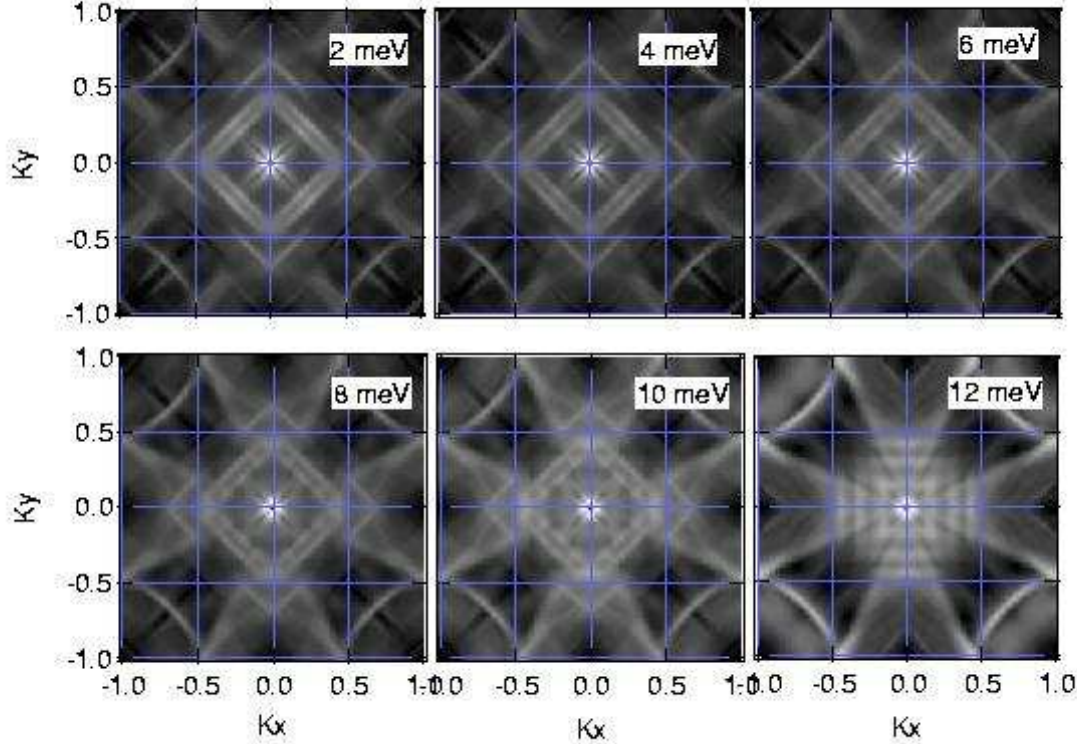


FIG. 2. Q-Maps constructed directly from convolution of measured ARPES spectral functions for a series of frequencies ω from 2 to 12 meV.

convolution spectrum is displayed. While there is considerable variation of relative intensities of the features with energy, the spectra are characterized by patterns of extended lines which do not shift significantly with ω . This is just the pattern expected from the convolution of the broadened ARPES spectra illustrated in Fig. 1. Since the ARPES spectral function is an extended arc, the convolution gives rise to a q-map consisting of similar arcs.

The ARPES spectra should show enhanced scattering at the special points found by Wang and Lee [7], due to a high local density of states. To understand the absence of these sharp peaks responsible for the STM features, it is necessary to calculate model theoretical spectra. Since STM measures a local density of states, the resulting q-map is itself a perturbative correction to the spectral function, which can be divided into a potential source term $V(q)$ and an electronic response. The source term is assumed to be some unknown function of the impurity distribution, NPS, etc., while the electronic response can be analyzed for the ‘spectrum’ of strongly coupled wave numbers. The response to a point impurity, considered as a superposition of magnetic and potential scatterers, has been studied in detail for d-wave superconductors [13]. A simple expression is possible when the scattering

is weak (Born limit):

$$\begin{aligned} \text{Im}(\delta G(\vec{q}, \omega)) &= \sum_{\vec{k}} \text{Im}(V_{\vec{q}} G(\vec{k} + \vec{q}, \omega) G(\vec{k}, \omega)) \\ &= V_{\vec{q}}'' \bar{\chi}'(\vec{q}, \omega) + V_{\vec{q}}' \bar{\chi}''(\vec{q}, \omega), \end{aligned} \quad (2)$$

where $V_{\vec{q}} = V_{\vec{q}}' + iV_{\vec{q}}''$, and similarly for $\bar{\chi}(\vec{q}, \omega)$ with response function

$$\bar{\chi}(q, \omega) = \sum_k G(k, \omega) G(k + q, \omega). \quad (3)$$

For comparison to ARPES, it is convenient to decompose $\bar{\chi}' = \bar{\chi}'_1 + \bar{\chi}'_2$, with

$$\bar{\chi}'_1(\vec{q}, \omega) = \sum_{\vec{k}} \text{Re}(G(\vec{k} + \vec{q}, \omega)) \text{Re}(G(\vec{k}, \omega)) \quad (4)$$

$$\bar{\chi}'_2(\vec{q}, \omega) = - \sum_{\vec{k}} \text{Im}(G(\vec{k} + \vec{q}, \omega)) \text{Im}(G(\vec{k}, \omega)), \quad (5)$$

The significance of this separation comes from the fact that the term $\bar{\chi}'_2$ can be expressed as a convolution of the ARPES spectral weight $A = -\text{Im}(G)/\pi$ with itself, and hence can be numerically reconstructed directly from the ARPES spectrum.

To account for the large broadening found in the ARPES spectra, the Green's function is calculated in an Eliashberg approach, with allowance for elastic scattering. To minimize pairbreaking effects [14], it is assumed that the elastic scattering is predominantly small-angle scattering ($V_{\vec{q}} = V_1\delta(\vec{q})$), which is not pairbreaking. (Strong small angle scattering has been postulated in a number of studies of the cuprates [15–20].) In this case, the superconducting state Green's function becomes [21,14]

$$G(\vec{k}, \omega) = \frac{\omega Z_{\vec{k}} + \xi_{\vec{k}}}{(\omega^2 - \Delta_{\vec{k}}^2)Z_{\vec{k}}^2 - \xi_{\vec{k}}^2} \quad (6)$$

with $\xi_{\vec{k}} = \epsilon_{\vec{k}} - \epsilon_F$,

$$Z_{\vec{k}} = 1 + \frac{\Sigma_{1,\vec{k}}}{\sqrt{\Delta_{\vec{k}}^2 - \omega^2}}, \quad (7)$$

$\Sigma_{1,\vec{k}} = n_I N_{\vec{k}}(0) |V_1|^2$, and a d-wave gap is assumed $\Delta_{\vec{k}} = \Delta_0(c_x - c_y)/2$. In the overdoped Bi-2212 sample, the measured gap $\Delta_0(0)$ is 15 meV. Fits to the superconducting state dispersion give $\Sigma_1 \simeq 20\text{meV}$ (the angle dependence of Σ is neglected). As $\text{Im}\Sigma$ appears to increase as doping is decreased, a value $\Sigma_1 = 30\text{meV}$ is assumed for comparison with STM results.

From Eq. 6, $G(\vec{k}, \omega)$ develops an imaginary part when $\omega > \Delta_{\vec{k}}$. Near this threshold, $Z_{\vec{k}} \sim i\Sigma_I^{el}/\sqrt{\omega^2 - \Delta_{\vec{k}}^2}$, and

$$A(\vec{k}, \omega) = \frac{\omega \Sigma_I^{el}/\pi}{(\xi_{\vec{k}}^2 + \Sigma_I^{el2})\sqrt{\omega^2 - \Delta_{\vec{k}}^2}} \quad (8)$$

if $\omega \geq \Delta_{\vec{k}}$. Thus, the spectral weight actually *diverges at the 'bright spots'*, the special points which satisfy both $\xi_{\vec{k}} = 0$ and $\tilde{\omega} = \Delta_{\vec{k}}$. (This is different from the clean limit ($Z_{\vec{k}} = 1$), where the spectral weight is proportional to the local density of states, which peaks at the bright spots.)

Figure 3 shows the corresponding constant energy maps of A at several binding energies, including a small pairbreaking [22], $\Sigma_2 = 0.5\text{meV}$, plus giving ω a small imaginary part, $\delta_\omega = 1\text{meV}$. The bright spots are clearly visible, while the accompanying arcs approximately superpose on the bare dispersion at all energies.

Once the Green's function is known, the STM susceptibility, Eq. 3, can be calculated. Figure 4 compares several different contributions to the q-map, comparing $\bar{\chi}'_2$ (a) with the full $\bar{\chi}'$ (b), and then combining $\bar{\chi}'$ with $\bar{\chi}''$. To estimate the importance of this contribution, it is assumed for illustrative purposes that $V'_q = \pm V''_q$ in Fig. 4c,d. It can be seen that the convolution term is dominated by the bright spots, and reproduces the patterns found in STM measurements. Inclusion of the additional terms modifies the details of the spectral function convolution, enhancing features from the nesting of FS

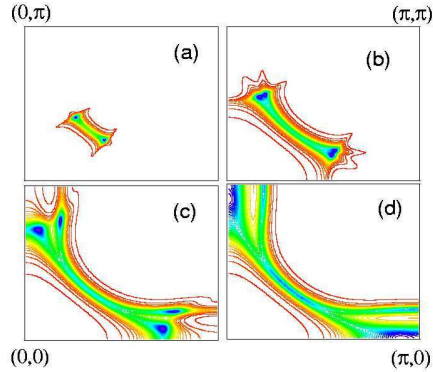


FIG. 3. Model ARPES spectral functions, at $\omega/\Delta = 0.2$ (a), 0.5 (b), 0.8 (c), and 1.0 (d).

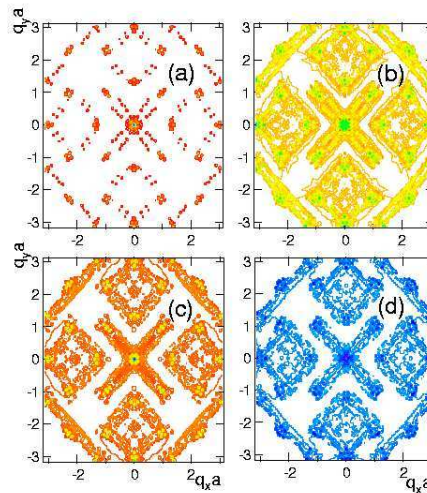


FIG. 4. Q-Maps for $\omega = 0.5 \Delta$, $\Sigma_1 = 0.003\text{eV}$: $-\bar{\chi}'_2$ (a), $-\bar{\chi}'$ (b), $-\bar{\chi}' + \bar{\chi}''$ (c), and $-\bar{\chi}' - \bar{\chi}''$ (d).

arcs while making the bright spots stand out somewhat less from the background, but does not lead to any significant shifts of spectral features.

Figure 5 shows a series of q-maps at various excitation energies ω , corresponding to the constant energy maps of Fig. 3. For simplicity, only the $\bar{\chi}'_2$ contribution is included. The general form of the resulting q-maps can readily be understood as a convolution of the bright spot peaks, exactly as in the experimental analysis [3]. The calculated positions of the bright spot convolutions are shown by the circles and squares in Fig. 5; at the higher energies, where the bilayer splitting is evident, the circles represent the stronger peaks associated with the antibonding band (nearer the VHS), the squares the weaker bonding band peaks. (Additional scattering from bonding to antibonding bright spots is automatically included in the calculated maps, but not illustrated by symbols.) While the resulting spectra include weak extended arcs, which shift little with ω , the bright spot features are quite

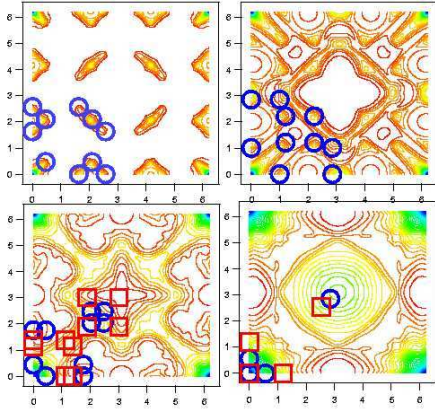


FIG. 5. Series of calculated STM q-maps corresponding to pairbreaking model of Fig. 3, for $\omega/\Delta =$ (a) 0.2, (b) 0.5, (c) 0.8, and (d) 1.0. Circles (squares) = calculated positions of convolution intensity corresponding to the most intense (second most intense) peaks in ARPES intensity. Note that in this and subsequent q-maps, the origin has been shifted with respect to Figs. 2 and 6.

prominent and strongly ω -dependent, yielding a q-map in good agreement with Ref. [2]. For $\omega > 0.5\Delta$, the agreement with experiment is less good. The spots from the bonding and antibonding bands overlap, leading to smoother spectra without clearly resolved bright spots. In contrast, the STM studies *do not find any features associated with the antibonding bands*, so the bonding band bright spots persist to higher energies.

While the experimental ARPES spectral functions show sharp quasiparticle peaks in the superconducting state, the bright spots are not clearly resolved. This can be understood as due to the finite energy resolution. Thus, Fig. 6a shows the result of averaging the MD spectra over the range $0 \leq \omega \leq 0.5\Delta_0$. The resulting strips of roughly constant intensity are in much better agreement with the measured ARPES spectra. Note that the experimental resolution in Fig. 1 is $\sim 15\text{meV} \sim \Delta_0$. The resulting convolution, Fig. 6b, is in good agreement with the experimental convolutions of Fig. 2.

There is one striking discrepancy between the model calculations and the STM maps: the ARPES spectra find a bilayer splitting while STM does not. In particular, model q-maps find both bilayer split bands, with the most intense feature coming from the (antibonding) band nearest the Van Hove singularity. On the other hand, the STM derived q-maps were inverted [3] to reconstruct the Fermi surface, and *only a single Fermi surface section was found*, corresponding to the bonding band. While the bilayer splitting is most easily observed in overdoped and Pb substituted samples, it is found [23,24] that in underdoped samples the bilayer splitting does not decrease, although the spectra broaden.

In conclusion, a detailed comparison of recent ARPES

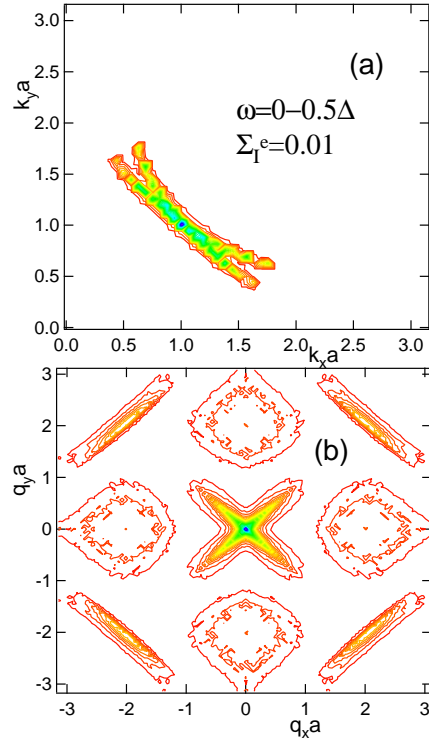


FIG. 6. Calculated ARPES (a) and STM q-maps (b), assuming limited energy resolution $\omega = 0 - 0.5\Delta$.

and STM measurements in BISCO has been provided. It is found that the most striking features of the STM results can be understood in terms of ‘bright spot’ quasiparticles, but that conclusive evidence will have to await higher resolution ARPES measurements. In the clean limit, the ARPES spectral weight of the bright spots has been estimated. In particular, it is predicted that the ARPES ‘peak’ feature is really an image of these dispersive bright spots, smeared into an extended streak by finite energy resolution. Residual discrepancies remain between the STM-derived and ARPES Fermi surfaces, in particular the absence of bilayer splitting in the STM results.

Acknowledgments: This work was begun while I was on sabbatical at Stanford. I thank Z.X. Shen, P. Bogdanov, A. Lanzara, J.C. Davis, A. Kapitulnik, and M. Greven for many stimulating conversations, and Z.X. Shen and P. Bogdanov for permission to use Figs. 3, 2.

-
- [1] C. Howald, *et al.*, Phys. Rev. **B67**, 014533 (2003); S.A. Kivelson, *et al.*, cond-mat/0210683.
 - [2] J.E. Hoffman, *et al.*, Science **297**, 1148 (2002).
 - [3] K. McElroy, *et al.*, Nature **422**, 592 (2003).

- [4] D. Podolsky, *et al.*, cond-mat/0204011.
- [5] A. Polkovnikov, *et al.*, Phys. Rev. B **65**, 220509 (2002).
- [6] J.H. Han, cond-mat/0206284.
- [7] Q.-H. Wang and D.-H. Lee, Phys. Rev. B **67**, 020511 (2003).
- [8] M.F. Crommie, J. El. Spectrosc. and Rel. Phenom. **109**, 1 (2000).
- [9] P.V. Bogdanov, *et al.*, Phys. Rev. Lett. **89**, 167002 (2002).
- [10] D.L. Feng, *et al.*, Phys. Rev. Lett. **86**, 5550 (2001).
- [11] A. Bansil and M. Lindroos, Phys. Rev. Lett. **83**, 5154 (1999).
- [12] P.V. Bogdanov, personal communication.
- [13] M.E. Flatté and J.M. Byers, in *Sol. St. Physics, Vol. 52*, ed. by H. Ehrenreich and F. Spaepen (Academic, San Diego, 1999), p. 138.
- [14] A.J. Millis, *et al.*, Phys. Rev. B **37**, 4975 (1988).
- [15] A.A. Abrikosov, Physica C **222**, 191 (1994).
- [16] E. Cappelluti and L. Pietronero, Phys. Rev. B **53**, 932 (1996).
- [17] M.L. Kuclic and R. Zeyher, Phys. Rev. B **49**, 4395 (1994).
- [18] M. Grilli and C. Castellani, Phys. Rev. B **50**, 16880 (1994).
- [19] G. Varelogiannis, *et al.*, Phys. Rev. B **54**, 6877 (1996).
- [20] E. Abrahams and C.M. Varma, Proc. Natl. Acad. Sci. **97**, 5714 (2000).
- [21] K. Maki, in *Superconductivity*, ed. by R.D. Parks, (Marcel Dekker, N.Y., 1969), p. 1035.
- [22] R.S. Markiewicz, unpublished.
- [23] D.L. Feng, *et al.*, Phys. Rev. B **65**, 220501 (2002).
- [24] Y.-D. Chuang, *et al.*, unpublished.